



# The influence of water chemistry on the radiolysis of the primary coolant water in pressurized water reactors

B. Pastina, J. Isabey, B. Hickel \*

Commissariat à l'Energie Atomique, CEA-Saclay, DSM/DRECAM/SCM URA 331 CNRS, Bâtiment 125, F-91191 Gif sur Yvette cedex, France

Received 9 April 1998; accepted 27 July 1998

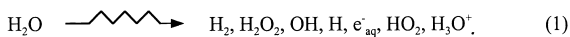
## Abstract

In order to study the radiolysis of PWRs primary coolant we irradiated several water samples containing hydrogen and boric acid in an experimental reactor. It was found that water decomposition to oxygen and to hydrogen peroxide is a threshold phenomenon depending on the experimental parameters such as the characteristics of the radiation and the water chemistry. An increase in temperature reduces the extent of water decomposition in presence of hydrogen. On the other hand, an increase of the boric acid concentration causes a higher decomposition. The minimum amount of molecular hydrogen used to inhibit the decomposition in our experiments was 0.23 ppm. Experiments with iron(III) and zinc nitrate dissolved in water showed that, in our conditions, zinc nitrate does not have any influence on water decomposition whereas iron(III) nitrate causes a greater decomposition. An experiment at pH = 7 (200°C) using <sup>7</sup>LiOH also showed an important formation of oxidizing products. © 1999 Elsevier Science B.V. All rights reserved.

PACS: 28.41.Fr

## 1. Introduction

The radiolysis of the primary coolant water in nuclear reactors is often related to corrosion problems. The interaction between the radiation and water forms molecular (H<sub>2</sub>, O<sub>2</sub>, H<sub>2</sub>O<sub>2</sub>) and radical (H, OH, e<sub>aq</sub><sup>-</sup>, HO<sub>2</sub>) species which participate to the general corrosion of the system

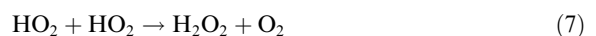


The main reactions taking place during water radiolysis are reported in Table 1. The stable products of water radiolysis are molecular hydrogen, oxygen and hydrogen peroxide. An excess of molecular hydrogen is dissolved in the primary coolant water of pressurized water reactors (PWR) in order to prevent the accumulation of oxidant products, such as oxygen and hydrogen perox-

ide, which are responsible for the corrosion of the primary system [1]. The molecular hydrogen participates to a chain reaction which recombines H, OH and H<sub>2</sub>O<sub>2</sub> back to water:



The chain reaction is propagated by the H atom and the OH radical, therefore the higher their concentration in water, the more efficient will be the recombination. Moreover, in the presence of hydrogen and of sufficient radical concentration, all traces of oxygen are reduced to H<sub>2</sub>O<sub>2</sub> and finally into water by reactions (2) and (3):

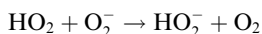


\* Corresponding author. Tel.: +33-1 69 08 51 26; fax: +33-1 69 08 66 40; e-mail: hickel@scm.saclay.cea.fr.

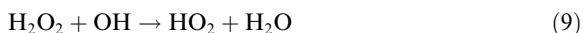
Table 1

The reaction scheme of the radiolysis of neutral water. The activation energies ( $E_a$  in  $\text{kJ moles}^{-1}$ ), the Arrhenius factor frequencies ( $A$  in  $\text{moles}^{-1} \text{dm}^3 \text{s}^{-1}$ ) as well as the rate constants ( $\text{moles}^{-1} \text{dm}^3 \text{s}^{-1}$ ) are extracted from the Rates<sup>®</sup> database [10]

Reactions	$A$	$E_a$	Rate constant
$e_{\text{aq}}^- + \text{H} (+\text{H}_2\text{O}) \rightarrow \text{H}_2 + \text{OH}^-$	$2.5 \times 10^{13}$	16.3	$3.4 \times 10^{10}$
$e_{\text{aq}}^- + e_{\text{aq}}^- (+2\text{H}_2\text{O}) \rightarrow \text{H}_2 + 2\text{OH}^-$	$5.9 \times 10^{13}$	22	$5.5 \times 10^9$
$e_{\text{aq}}^- + \text{OH} \rightarrow \text{OH}^-$			$3 \times 10^{10}$
$e_{\text{aq}}^- + \text{H}_3\text{O}^+ \rightarrow \text{H} + \text{H}_2\text{O}$	$8.9 \times 10^{12}$	14.5	$2.3 \times 10^{10}$
$e_{\text{aq}}^- + \text{H}_2\text{O}_2 \rightarrow \text{OH} + \text{OH}^-$	$7.3 \times 10^{11}$	10.0	$1.3 \times 10^{10}$
$e_{\text{aq}}^- + \text{O}_2 \rightarrow \text{O}_2^-$	$1.6 \times 10^{12}$	11.0	$1.9 \times 10^{10}$
$e_{\text{aq}}^- + \text{O}_2^- \rightarrow \text{O}_2^{2-}$			$1.3 \times 10^{10}$
$e_{\text{aq}}^- + \text{H}_2\text{O} \rightarrow \text{H} + \text{OH}^-$	$3.6 \times 10^8$	31.7	$1.0 \times 10^3$
$\text{OH} + \text{OH} \rightarrow \text{H}_2\text{O}_2$			$5.5 \times 10^9$
$\text{OH} + \text{H}_2\text{O}_2 \rightarrow \text{H}_2\text{O} + \text{HO}_2$	$8.5 \times 10^9$	14.0	$2.7 \times 10^7$
$\text{OH} + \text{H}_2 \rightarrow \text{H}_2\text{O} + \text{H}$	$8.3 \times 10^{10}$	19.0	$3.9 \times 10^7$
$\text{OH} + \text{HO}_2 \rightarrow \text{H}_2\text{O} + \text{O}_2$			$1.1 \times 10^{10}$
$\text{OH} + \text{O}_2^- \rightarrow \text{OH}^- + \text{O}_2$	$1.4 \times 10^{13}$	17.6	$1.1 \times 10^{10}$
$\text{H}_3\text{O}^+ + \text{OH}^- \rightarrow 2\text{H}_2\text{O}$			$3 \times 10^{10}$
$\text{H} + \text{H} \rightarrow \text{H}_2$			$5 \times 10^9$
$\text{H} + \text{OH} \rightarrow \text{H}_2\text{O}$			$7.0 \times 10^9$
$\text{H} + \text{H}_2\text{O}_2 \rightarrow \text{H}_2\text{O} + \text{OH}$	$3.7 \times 10^{10}$	16.4	$5.0 \times 10^7$
$\text{H} + \text{HO}_2 \rightarrow \text{H}_2\text{O}_2$			$2 \times 10^{10}$
$\text{H} + \text{O}_2 \rightarrow \text{HO}_2$	$1.4 \times 10^{11}$	6.2	$2.1 \times 10^{10}$
$\text{H} + \text{OH}^- \rightarrow e_{\text{aq}}^- + \text{H}_2\text{O}$	$1.3 \times 10^{14}$	38.4	$2.2 \times 10^7$
$\text{HO}_2 + \text{HO}_2 \rightarrow \text{H}_2\text{O}_2 + \text{O}_2$	$4.0 \times 10^9$	20.6	$9.8 \times 10^5$
$\text{HO}_2 + \text{O}_2^- \rightarrow \text{HO}_2^- + \text{O}_2$			$9.7 \times 10^7$
$\text{H}_2\text{O}_2 + \text{HO}_2 \rightarrow \text{H}_2\text{O} + \text{O}_2 + \text{OH}$			0.5
$\text{O}_2^- + \text{H}_3\text{O}^+ \rightarrow \text{HO}_2 + \text{H}_2\text{O}$			$5 \times 10^{10}$
$\text{O}_2^- + \text{H}_2\text{O}_2 \rightarrow \text{OH} + \text{OH}^- + \text{O}_2$			0.13
$\text{H}_2\text{O} (+\text{H}_2\text{O}) \rightleftharpoons \text{H}_3\text{O}^+ + \text{OH}^-$			$\text{p}K = 14$
$\text{H}_2\text{O}_2 (+\text{H}_2\text{O}) \rightleftharpoons \text{H}_3\text{O}^+ + \text{HO}_2^-$			$\text{p}K = 11.7$
$\text{HO}_2 (+\text{H}_2\text{O}) \rightleftharpoons \text{H}_3\text{O}^+ + \text{O}_2^-$			$\text{p}K = 4.8$



If the oxygen concentration is too high, all H radicals are scavenged by reaction (6) which has a much higher rate constant than reaction (3) which is thus stopped. Therefore, it is primordial to avoid such oxygen accumulations. The accumulation of hydrogen peroxide is also to avoid because, although it takes part to the recombination mechanism (3) it can be a source of oxygen by reaction (9) followed by reactions (7) or (8)



Thus, hydrogen peroxide and oxygen are two species linked to each other and they both inhibit the chain reaction if their concentration is too high. The mechanism of water radiolysis implies several other reactions (see Table 1) and it is influenced by the experimental parameters such as the radiation characteristics, the temperature, and the chemical composition of the cooling water. It is very difficult to foresee, without experimental data, the overall effect of these parameters. That is why we decided to study the radiolysis of water

samples under different experimental conditions. In this paper we present the data concerning water radiolysis as a function of the boric acid concentration. We also studied the influence of the hydrogen concentration in water. Water can also contain impurities such as iron cations coming from the corrosion and nitrate anions coming from the radiolysis of water containing some traces of air. We compared the effect of iron to the results obtained with the zinc cation, which is becoming a very important species for the primary water because it has been shown to decrease the radioactivity build-up in the crud [2]. Finally, we irradiated different aqueous solutions of boric acid at  $\text{pH} = 7$  at  $200^\circ\text{C}$ , using  $^7\text{LiOH}$  as the pH control agent like in PWRs.

## 2. Experimental

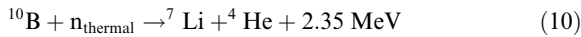
### 2.1. Preparation of the samples

Triply distilled water is used to prepare the samples to be irradiated. Each sample contains different amounts of boric acid. Natural boric acid, “NBA” (Aldrich, 99.999%) and  $^{10}\text{B}$ -enriched (99.5% of  $^{10}\text{B}$ )

boric acid, “EBA” (Eagle Picher GmbH, chemical purity: 99.94%) were used as received. The pH of the samples containing NBA varied from 3 to 5.5 whereas the pH of the samples containing EBA was close to 5.5. The high temperature pH values were calculated with the MULTEQ<sup>®</sup> code at CEA/Fontenay aux Roses. <sup>7</sup>LiOH (isotopic enrichment: 99.999%) from Euriso-Top (minimum chemical purity 99.5%) was used in one experiment to adjust the pH of the samples (pH = 7 at 200°C). Argon (99.9995%, from Air Liquide) is bubbled in each sample during 10 min and then molecular hydrogen (99.9995%, from Air Liquide) is bubbled during 50 min. The amount of gas bubbled is checked by a flow control device. It is verified by mass spectrometry that each sample is hydrogen-saturated ( $7.8 \times 10^{-4}$  moles dm<sup>-3</sup> at 20°C) after this treatment. A cylindrical quartz ampoule (diameter = 0.008 m and height = 0.1 m) is previously flushed with hydrogen to remove all traces of air. The ampoule is half-filled with the solution and the remaining head-space is filled with hydrogen at atmospheric pressure. The ampoules are immediately sealed after the filling.

## 2.2. Irradiation facility

All the irradiations took place at the ISIS reactor at the CEA CE/Saclay. ISIS is an experimental reactor whose core is composed by enriched UO<sub>2</sub> rods. The fission reaction delivers a gamma radiation as well as fast neutrons. As the core is immersed in a water pool, part of the fast neutrons are thermalised by elastic collision with the hydrogen atoms of water. The thermal neutrons,  $n_{\text{thermal}}$ , are captured by the isotope 10 of boron, <sup>10</sup>B contained in the samples as boric acid, following the reaction



We will refer to the Li recoils, <sup>7</sup>Li, and alpha particles, <sup>4</sup>He, as the <sup>10</sup>B(n,α)<sup>7</sup>Li radiation. The mean Linear Energy Trasfer (LET) of the lithium and helium recoils is calculated by the program TRIM<sup>®</sup> from their kinetic energy and it is 203 keV μm<sup>-1</sup>. The dose depends on the <sup>10</sup>B concentration in water following the relationship

$$\text{dose rate } ^{10}\text{B}(n, \alpha)^7\text{Li} = F I_0 (1 - e^{-n\sigma x}) 2.35 \times 10^6 \quad (11)$$

where  $I_0$  is the initial thermal neutron flux,  $n$  is the number of <sup>10</sup>B atoms per m<sup>3</sup>,  $\sigma$  is the thermal neutron absorption cross section of <sup>10</sup>B (3837 barns),  $x$  the thickness of the samples and  $F$  is a factor that takes into account the cylindrical shape of the container.

The samples are irradiated during 60 min in a sample holder located in the reactor’s pool. The temperature of the irradiation is controlled by a heating device installed in the sample holder. After the irradiation, the samples are left about 60 additional hours in the sample holder at room temperature in order to allow the radioactivity coming from the oven to decrease. The gamma dose during the storage is negligible. Table 2 shows the characteristics of the reactor at the location where the samples were irradiated, as well as some of the relevant PWR characteristics. The position of the samples has been chosen to be in the first periphery of the core such that the effect of the fast neutrons is small (about 10% of the total neutron flux) compared to the thermal neutrons and gamma flux.

### 2.2.1. The temperature control

The temperature of the samples is regulated by a special sample holder (shown in Fig. 1) designed for this particular experiment. This water-tight irradiation device consists of a double-shell stainless steel cylinder about 6 m long and 0.4 m of outer diameter. The inner wall includes the heating elements. These are simple electric resistors as well as ten thermocouples uniformly distributed along the walls. Half of them are for the heat control and half are for the heat regulation. Between the inner and the outer walls a nitrogen jacket at atmospheric pressure ensures the uniform distribution of heat throughout the oven. The sample holder is made of aluminum in order to avoid a too strong activation and too long radioactive decays. The sample holder can host eight ampoules, four in its upper half and four in its bottom part. The samples are irradiated at the level of maximum flux of the reactor. The sample holder also has a radiobiological protection. Electrical racks are used to set and monitor the temperature of the oven. The calibration has been performed using eight thermocouples situated at the location of each ampoule. It has been checked that there are not any axial or cross gradients of temperature.

Table 2  
Characteristics of the radiation at the location of the samples and comparison with the Ringhals PWR reactor [15]

	ISIS experiments	PWR
Gamma dose rate	8.46 kGy h <sup>-1</sup> (0.023 W g <sup>-1</sup> )	$5 \times 10^3$ kGy h <sup>-1</sup> (1.45 W g <sup>-1</sup> )
Thermal neutron fluence	$1.4 \times 10^{15}$ n m <sup>-2</sup> s <sup>-1</sup>	$2.5 \times 10^{18}$ n m <sup>-2</sup> s <sup>-1</sup>
Fast neutron fluence	$1.3 \times 10^{14}$ n m <sup>-2</sup> s <sup>-1</sup>	$7.5 \times 10^{18}$ n m <sup>-2</sup> s <sup>-1</sup>
Fast neutron dose rate	( $8.45 \times 10^{-5}$ W g <sup>-1</sup> )	(4.85 W g <sup>-1</sup> )
Thermal power MW	0.07	2800
Temperature	30, 100, 200°C	from 280 to 320°C

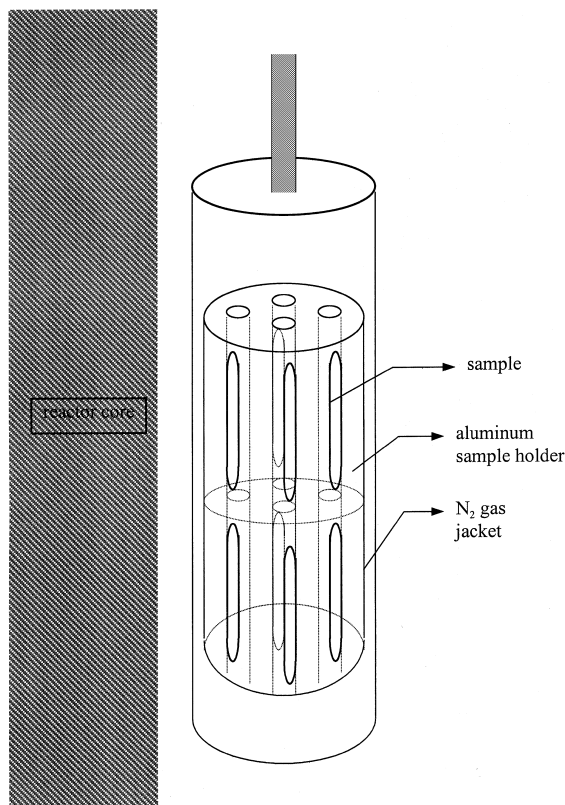


Fig. 1. The ISIS irradiation device located in the pool. The shaded area represents part of the reactor core's wall. The electric resistors to heat the samples are not shown for clarity.

### 2.2.2. The dosimetry

The neutron dosimetry was carried by neutron counting on a cobalt foil. In order to differentiate the fast neutron flux from the thermal and epithermal flux, a cadmium foil surrounded some of the cobalt detectors. As cadmium stops all neutrons with an energy lower than 0.6 eV, the ratio between the cobalt–cadmium detectors and the cobalt detectors gives the ratio between the fast neutrons and the total neutron flux. This ratio was 0.09. The gamma dosimetry was carried with a graphite differential calorimeter. The error on both the neutron and the gamma dosimetry does not exceed 5%.

### 2.3. Analysis of the samples

The gas phase is extracted with a vacuum Toeppler pump. The gas are analyzed by mass spectrometry to dose  $H_2$ ,  $O_2$ , Ar and  $N_2$ . None of the samples contained carbon dioxide after the irradiation. The pressure of gas in the samples is measured by a high-precision pressure gauge. The liquid phase is analyzed by the Ghormley method [3] to dose  $H_2O_2$ . Knowing the dose and the

concentration of  $O_2$  and  $H_2O_2$  (in moles  $kg^{-1}$ ) we can calculate the experimental yields  $G(O_2)$  and  $G(H_2O_2)$

$$G = \text{concentration/dose} \quad (12)$$

where  $G$  is the radiolytic yield in moles  $J^{-1}$  and the dose is the total dose in Gy. By applying the material balance we calculate the water decomposition yield (1 mole  $J^{-1} = 9.65 \times 10^6$  molecules  $(100 \text{ eV})^{-1}$ )

$$G(-H_2O) = 2G(O_2) + 2G(H_2O_2) \quad (13)$$

## 3. Results and discussion

### 3.1. The influence of the boric acid concentration

Boric acid is used in the primary water of PWR nuclear reactors as a water soluble thermal neutron absorber. Its concentration is maximum at the beginning of the fuel life (1500 ppm of natural boron) and it decreases to 0 ppm when the fuel is spent out. At the shutdown for the refueling of the reactor, boric acid is also injected at high concentration in order to absorb all the thermal neutrons (10) and stop the fission reaction. The boric acid concentration is directly linked to the LET of the radiation by relation (11). An increase of the  $^{10}B(n,\alpha)^7Li$  dose causes an increase of the Global LET, GLET, defined as

$$GLET = LET_\gamma \times R_\gamma + LET_{B(n,\alpha)Li} \times (1 - R_\gamma) \quad (14)$$

where  $LET_\gamma$  and  $LET_{B(n,\alpha)Li}$  are the Linear Energy Transfer of the gamma radiation and the  $^{10}B(n,\alpha)^7Li$  radiation, respectively, and  $R_\gamma$  is the fraction of the total dose due to the gamma radiation. The GLET is dependent on the ratio between the dose of the  $^{10}B(n,\alpha)^7Li$  radiation and the  $\gamma$  radiation,  $^{10}B(n,\alpha)^7Li/\gamma$ . The influence of the radiation LET on the mechanism of water radiolysis in nuclear reactors is studied elsewhere [1,4,5]. Briefly, a low LET radiation, such as the gamma radiation ( $0.23 \text{ keV } \mu\text{m}^{-1}$ ), produces in water more radical products ( $e_{aq}^-$ , H, OH) than molecular products ( $H_2O_2$ ,  $H_2$ ) whereas a high-LET radiation, such as the  $^{10}B(n,\alpha)^7Li$  radiation ( $203 \text{ keV } \mu\text{m}^{-1}$ ), acts in the opposite way [6]. The experimental results show that a low LET radiation helps the recombination mechanism because of the higher radical concentrations which increase the length of the chain reaction (4). A high-LET radiation inhibits the recombination mechanism because of the higher concentration of hydrogen peroxide which slows down and eventually stops the chain reaction as it is explained in the introductory part. Schematically, we can say that a low-LET radiation, like the gamma rays, favors the recombination of the radiolysis products of water whereas a high-LET radiation, like alpha rays, favors the formation of molecular oxygen, hydrogen and hydrogen peroxide and so it leads to the decomposition

of water. Thus, the extent of water decomposition is not the same in every part of the coolant circuit, depending on the local ratio  $[^{10}\text{B}(n,\alpha)^7\text{Li} + \text{fast neutrons}]/\gamma$ . This ratio is variable in space because it depends on the distance from the core and in time because it depends on the age of the core to which is linked the boric acid concentration. Fig. 2 shows the effect of the  $^{10}\text{B}$  concentration on water radiolysis at three different temperatures: 30°C, 100°C and 200°C. The radiolytic yield of oxygen,  $G(\text{O}_2)$  and of hydrogen peroxide,  $G(\text{H}_2\text{O}_2)$ , formed by water radiolysis are expressed in moles  $\text{J}^{-1}$ . As we can see, at room temperature there exists a threshold in water decomposition as a function of the  $^{10}\text{B}$  concentration. At low concentration,  $\text{O}_2$  and  $\text{H}_2\text{O}_2$  do not form in measurable quantities but above the threshold there is a rapid increase of these products. As

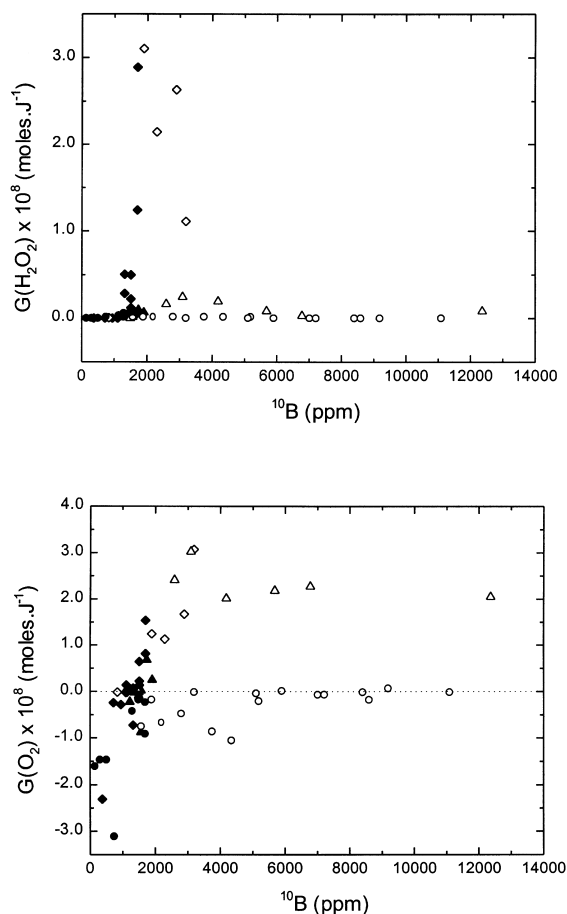


Fig. 2. The effect of  $^{10}\text{B}$  concentration on the water radiolysis products on  $G(\text{O}_2)$  and  $G(\text{H}_2\text{O}_2)$  in moles  $\text{J}^{-1}$ . ( $\blacklozenge$ ) 30°C NBA, ( $\diamond$ ) 30°C EBA, ( $\blacktriangle$ ) 100°C NBA, ( $\triangle$ ) 100°C EBA, ( $\bullet$ ) 200°C NBA, ( $\circ$ ) 200°C EBA. NBA: Natural Boric Acid (19.8% of  $^{10}\text{B}$ ), and EBA: Enriched Boric Acid (99.5% of  $^{10}\text{B}$ ).

the temperature increases, the threshold is shifted towards a higher  $^{10}\text{B}$  concentration and at 200°C it is not visible in the range of  $^{10}\text{B}$  concentration used. The existence of this threshold and its evolution with the temperature can be explained by the mechanism of water radiolysis in the presence of hydrogen which is detailed elsewhere [1,4,5]. Briefly, an increase of the  $^{10}\text{B}$  concentration leads to an increase of the Global LET because the ratio  $^{10}\text{B}(n,\alpha)^7\text{Li}/\gamma$  increases. An increase of the LET implies an increase of molecular products formed by radiolysis and a decrease of the radical products which has a negative effect on the recombination mechanism. On the other hand, a temperature increase has a beneficial effect on this mechanism because of three factors ([4] and references therein). First of all, the radical yields increase and the molecular yields decrease with temperature. Moreover, the kinetics of the chain reaction (2) and (3) is more favored by a temperature increase than that of the reactions leading to the formation of oxygen and of hydrogen peroxide (9), (7), (8). Finally, a rise in the temperature increases the amount of hydrogen dissolved in water because of the increase of the hydrogen partial pressure in the samples. For these reasons the decomposition threshold of water under radiolysis is shifted towards higher  $^{10}\text{B}$  concentrations when we raised the temperature between 30°C and 200°C. In Fig. 2, a negative oxygen radiation yield,  $G(\text{O}_2)$ , is observed for some samples containing low  $^{10}\text{B}$  concentrations. These samples contained traces of oxygen coming from an air entry during the ampoule-sealing procedure. We calculated the initial oxygen concentration from the nitrogen measured by mass spectroscopy after the irradiation. For these samples we compared the initial oxygen concentration and the final concentration after the irradiation and we found that there had been a net oxygen consumption. This is a direct effect of the recombination mechanism in presence of hydrogen. As a matter of fact, at low LET, which means low  $^{10}\text{B}$  concentration, oxygen is reduced to hydrogen peroxide by the radicals through reactions (5)–(8). Hydrogen peroxide recombines with hydrogen by the chain reaction (2) and (3) to form water. The negative oxygen formation yields are then explained at low LET. Other samples, at higher  $^{10}\text{B}$  concentrations, contained traces of air with but the oxygen yields were all positive because the radical concentration was not high enough to reduce the oxygen and the hydrogen peroxide back to water. These experiments showed that it is possible to control small increases of oxygen concentration in water providing that the LET of the radiation is low enough and that there is sufficient hydrogen to recombine with the excess of oxygen.

### 3.1.1. The influence of $^{10}\text{B}$ -EBA

Part of the samples were irradiated using  $^{10}\text{B}$ -EBA (in Fig. 2), and part using NBA. In spite of a 5-fold

difference in the boric acid concentration, the experiments showed the same  $^{10}\text{B}$  concentration at the threshold. Therefore boric acid does not have any chemical effect on the water decomposition but only a nuclear effect due to the radiation issued from the  $^{10}\text{B}$  reaction with thermal neutrons. Thus,  $^{10}\text{B}$ -EBA can be safely used, from the radiolysis point of view, to replace NBA in PWR reactors.

### 3.2. The influence of the hydrogen concentration

Hart et al. [7] have found that dissociation of water in boric acid solutions under reactor irradiation could be suppressed by initial hydrogen in the coolant. In French PWRs the hydrogen concentration range is between 20 and 30  $\text{cm}^3 \text{kg}^{-1}$  of water NTP (1.8–2.7 ppm). Hydrogen is very successful to reduce the corrosion both in PWRs and in BWRs, nevertheless it presents few drawbacks. First of all, it is known to enhance the stress corrosion cracking of the steam generator and to damage the zircaloy fuel claddings [8]. Moreover, hydrogen has to be eliminated from the circuit before the refueling, therefore the less hydrogen is dissolved, the shorter will be the dehydrogenation time, leading to a certain economic benefit. The question that arises is: what is the minimum hydrogen concentration to dissolve in order to avoid water decomposition? Different concentrations of hydrogen were studied at 200°C to find the minimum amount needed to inhibit water decomposition. In Fig. 3

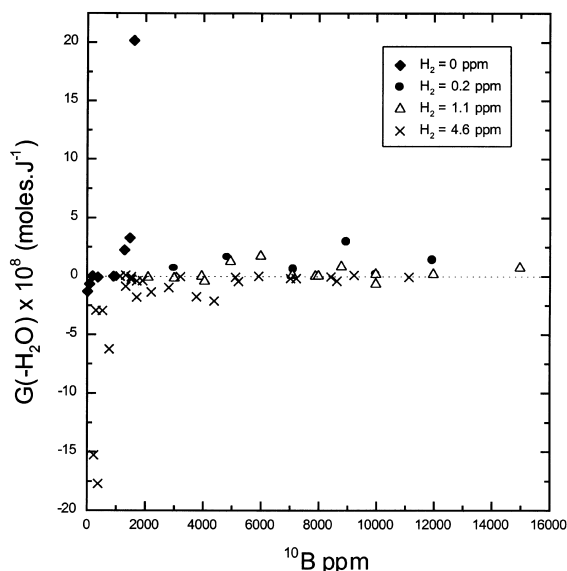


Fig. 3. The effect of different hydrogen concentrations at 200°C as a function of the  $^{10}\text{B}$  concentration.  $G(-\text{H}_2\text{O})$  is calculated from Eq. (13) and is expressed in moles  $\text{J}^{-1}$ .  $^{10}\text{B}$ -EBA was used for concentrations higher than 2000 ppm.

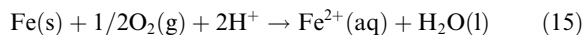
we show the experimental results obtained at 200°C with 0, 0.23, 1.15 and 4.6 ppm of hydrogen in water. Fig. 3 shows that water decomposes readily in the absence of hydrogen. On the other hand, the addition of 0.23 ppm of hydrogen and more inhibits almost completely the formation of oxygen and of hydrogen peroxide. Another experiment with low hydrogen concentrations has been performed at the Belleville French nuclear plant [8]. In this in-pile experiment, the hydrogen concentration was lowered to 3.6  $\text{cm}^3 \text{kg}^{-1}$  NTP (0.3 ppm) without any significant increase of the radiolysis products concentration. Our experimental results, together with theirs, show that hydrogen can be safely reduced by a factor 2 or 3 in the primary cooling water but it is important to maintain a comfortable excess to prevent any accidental accumulation of oxidizing product.

### 3.3. The influence of zinc nitrate in water

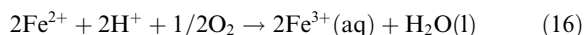
Zinc injection in BWR water has been found to suppress the  $^{60}\text{Co}$  and  $^{58}\text{Co}$  incorporation in stainless steel surface oxide, which reduces their activity build-up efficiently [2]. The mechanism of the zinc action has not been yet fully clarified. The usual zinc concentration added to BWR is around 10 ppb. It is nowadays necessary to study the action of this cation on the mechanism of water radiolysis. We chose the nitrate ion as the zinc counterion because it can be present as a secondary product of the radiolysis of water containing some traces of air or nitrogen. We added 2 ppm of  $\text{Zn}(\text{NO}_3)_2$  to our samples already containing boric acid and hydrogen. We irradiated these solutions at 30°C. Fig. 4 compares the water decomposition yield in the absence and in the presence of 2 ppm of  $\text{Zn}(\text{NO}_3)_2$ . Both series of samples are  $\text{H}_2$ -saturated at 20°C. As we can see, the threshold with  $\text{Zn}(\text{NO}_3)_2$  is the same as that of the blank samples. Therefore, at this concentration of  $\text{Zn}(\text{NO}_3)_2$  neither the nitrate ion, nor the zinc ion seem to have any effect on the recombination mechanism of water.

### 3.4. The influence of iron nitrate in water

Iron is a typical metallic impurity found in the primary circuit coming from the corrosion of stainless steels. The oxidizing reaction on the surface of metals releases only ferrous ions as the ferric iron release is thermodynamically unfavorable at high temperature [9]



The ferrous ions are then oxidized into ferric ions either by water



or by the oxidizing radiolysis products such as OH and  $\text{H}_2\text{O}_2$  and  $\text{HO}_2$ :

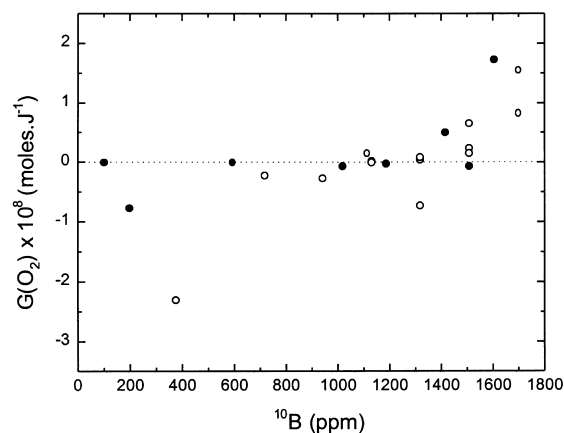
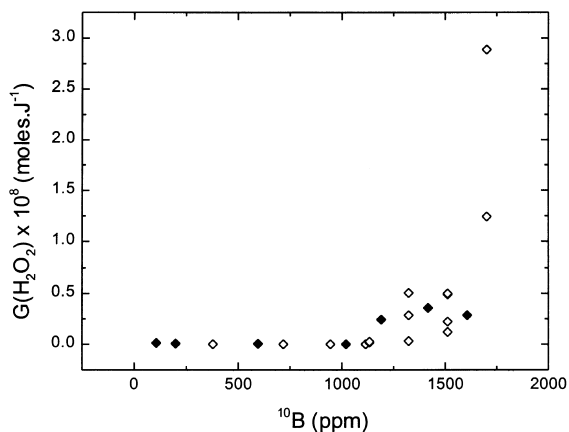
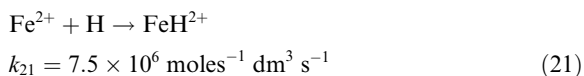
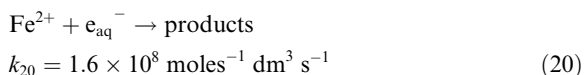
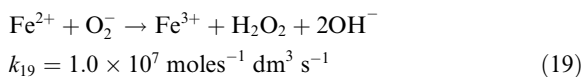
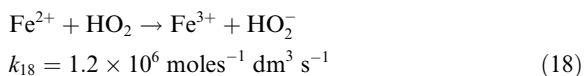
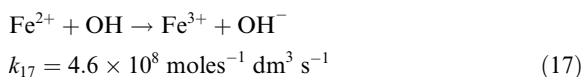


Fig. 4. The effect of  $Zn(NO_3)_2$  at 30°C on the hydrogen peroxide and oxygen yields expressed in moles  $J^{-1}$ . Solid symbols are for 2 ppm of  $Zn(NO_3)_2$  and open symbols are for blank solutions.



The room temperature rate constants,  $k$ , are extracted from the database Rates<sup>®</sup> [10].

The typical iron concentration in water should not exceed few ppb [11]. We studied the behavior of water samples containing hydrogen, boric acid and 2 ppm of  $Fe(NO_3)_3$ . The samples are irradiated at 30°C. In Fig. 5 we compare the threshold obtained with  $Fe(NO_3)_3$  to that of the blank samples. As it appears from Fig. 4, the nitrate ion does not seem to have any effect (at this concentration) on water radiolysis, therefore the difference between the two thresholds in Fig. 5 is probably due to the ferric ion. At this concentration, this ion reacts with the different species formed by water radiolysis:

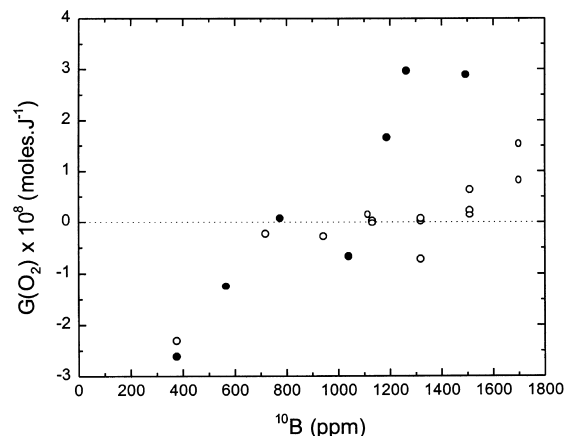
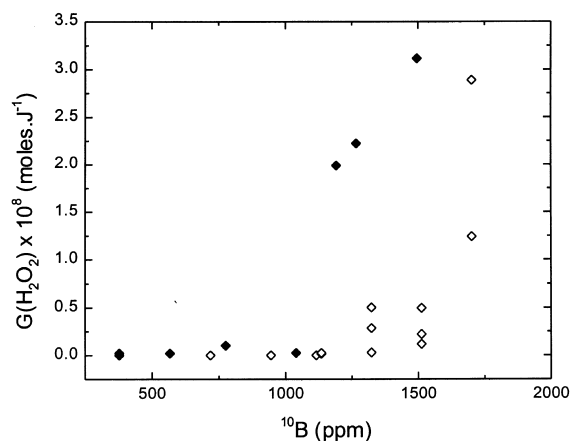


Fig. 5. The effect of  $Fe(NO_3)_3$  at 30°C on the hydrogen peroxide and oxygen yields expressed in moles  $J^{-1}$ . Solid symbols are for 2 ppm of  $Fe(NO_3)_3$  and open symbols are for blank solutions.

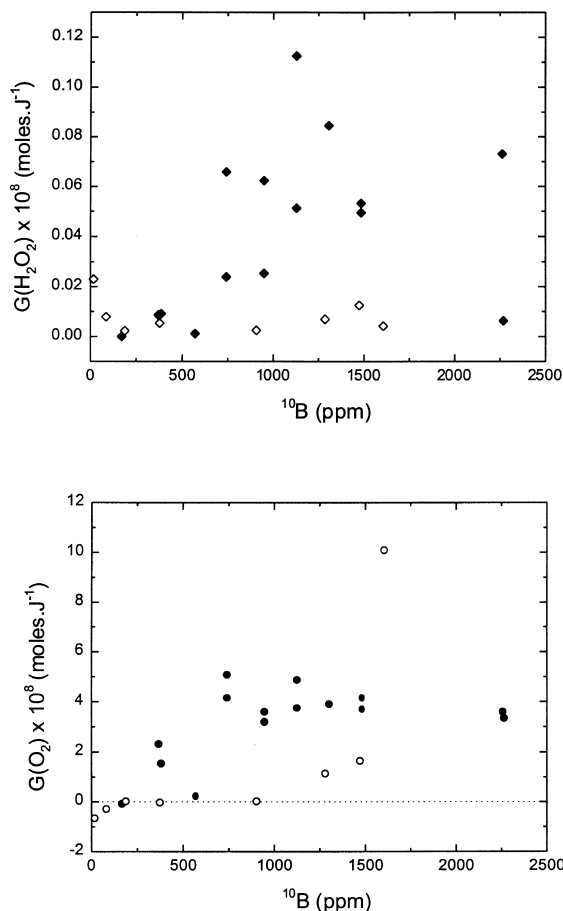
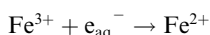
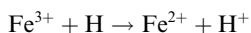


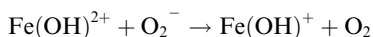
Fig. 6. The effect of  ${}^7\text{LiOH}$  on hydrogen peroxide and oxygen yields in moles  $\text{J}^{-1}$ . The temperature of the irradiation is  $200^\circ\text{C}$ . The solutions are argon-saturated. The  $\text{LiOH}$  concentrations were calculated by the code MULTEQ<sup>®</sup>. Solid symbols are for the solution at  $\text{pH}=7$  using  $\text{LiOH}$  and open symbols are for blank solutions.



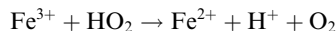
$$k_{22} = 6 \times 10^{10} \text{ moles}^{-1} \text{ dm}^3 \text{ s}^{-1} \quad (22)$$



$$k_{23} < 2 \times 10^6 \text{ moles}^{-1} \text{ dm}^3 \text{ s}^{-1} \quad (23)$$



$$k_{24} = 1.5 \times 10^8 \text{ moles}^{-1} \text{ dm}^3 \text{ s}^{-1} \quad (24)$$



$$k_{25} = 2 \times 10^4 \text{ moles}^{-1} \text{ dm}^3 \text{ s}^{-1} \quad (25)$$

These reactions, together with reactions (17)–(21) scavenge part of radicals so that the mechanism of water recombination is less efficient. It is therefore important to keep the ferric and the ferrous ion concentration as low as possible. It is very difficult to foresee what will be the effect of these impurities at higher temperature without experimental data.

### 3.5. The influence of lithium hydroxide in water

It has been shown that the optimum pH value for water of the primary circuit is around 7 at  $300^\circ\text{C}$  [11]. The pH control agent of most PWRs is lithium hydroxide ( ${}^7\text{LiOH}$ ). It has been proved, though, that lithium hydroxide enhances the zircaloy cladding corrosion and the Stress Corrosion Cracking (SCC) of steam generator tubes [12]. The maximum lithium concentration at the beginning of the reactor cycle is about 2.2 ppm. We present here a preliminary result about the influence of this chemical agent on water radiolysis. Two series of irradiations were performed at  $200^\circ\text{C}$  at constant pH ( $\text{pH}=7$  at  $200^\circ\text{C}$ ). The pH was fixed for each sample by calculation of the suitable  ${}^7\text{LiOH}$  concentration as a function of the boric acid concentration. The code MULTEQ<sup>®</sup> was used for these calculations at the CEA/Fontenay aux Roses. In order to compare the thresholds of water decomposition in Fig. 3 with that at constant  $\text{pH}_{200}=7$  we operated in the absence of hydrogen, saturating the solution with argon. The results are shown in Fig. 6. Table 3 shows the different boric acid and lithium hydroxide concentrations used. As we can see, at fixed pH the threshold shifts towards lower  ${}^{10}\text{B}$  concentrations. That is to say that water decomposes more in the presence of  $\text{LiOH}$ . There are different possible interpretations of this experimental result. Besides an impurity effect, which is the most plausible explanation, it is fair to take into consideration a pH effect or a  $\text{Li}^+$  effect. Nevertheless, the  $\text{Li}^+$  ion is not likely to play any role in the mechanism of hydrogen recombination since it does not react with the radicals formed during water radiolysis. On the other hand, the pH of the samples without  $\text{LiOH}$  is situated between 4 and 5.5 therefore there is not a big pH difference between the solutions irradiated at  $\text{pH}=7$ . In this range of pH, the primary yields do not change [13]. Among all chemical

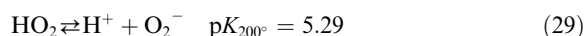
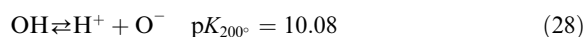
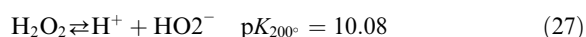
Table 3

Boric acid and  ${}^7\text{LiOH}$  concentrations in moles  $\text{kg}^{-1}$  of water in order to achieve a  $\text{pH}=7$  at  $200^\circ\text{C}$ . The  ${}^7\text{LiOH}$  concentrations were calculated using the MULTEQ<sup>®</sup> code at CEA/DTA/SCECF

$\text{H}_3\text{BO}_3$	0.09	0.2	0.3	0.4	0.5	0.6	0.7
${}^7\text{LiOH}$	$1.4 \times 10^{-3}$	$8.0 \times 10^{-3}$	$2.4 \times 10^{-2}$	$8.1 \times 10^{-2}$	$1.3 \times 10^{-1}$	$1.8 \times 10^{-1}$	$2.3 \times 10^{-1}$



equilibria, the only one that can be affected in this range of pH is reaction 27:



The high temperature p*K* values are calculated from Elliot et al. [14]. An increase in pH involves a greater fraction of O<sub>2</sub><sup>-</sup> radical anions which have a particularly negative effect on the recombination mechanism. These species scavenge the OH radicals to form oxygen following the reaction



This reaction involves the formation of molecular oxygen which is a chain breaker. However, at the moment, we cannot explain fully the increased decomposition in the presence of LiOH by this mechanism. The presence of impurities (Cl<sup>-</sup>, F<sup>-</sup>, Hg, Na, Pb and Zn) in <sup>7</sup>LiOH which scavenge part of the radicals could explain this result. Numerical simulations of water radiolysis are planned.

#### 4. Conclusion

In this paper we showed that the <sup>10</sup>B concentration is one of the key parameters for water radiolysis. An increase of the boric acid concentration leads to a higher <sup>10</sup>B(n,α)<sup>7</sup>Li dose, which has a negative impact on the mechanism of water recombination with hydrogen. Thus water is more exposed to decomposition by radiolysis at the beginning of the fuel cycle, when the boric acid concentration is maximum. Prior to the shut down operations, boric acid is also injected to stop the fission reaction, therefore at this moment too, water is more likely to be radiolytically decomposed due to the high dose of <sup>10</sup>B(n,α)<sup>7</sup>Li radiation. On the other hand, water decomposition is independent of the boric acid concentration for the same amount of <sup>10</sup>B: <sup>10</sup>B-EBA can be used without any consequences on water radiolysis. Concerning the hydrogen concentration used to avoid water radiolysis, previous experiments have shown that the actual concentration used in PWR reactors is largely in excess. Our experiments confirm these results. On the other hand, it is necessary to keep the impurity level as low as possible, especially the iron(III) concentration, in order to avoid any interference with the recombination mechanism. The nitrate ion (NO<sub>3</sub><sup>-</sup>) and the zinc cation (Zn<sup>2+</sup>) do not seem to be critical parameters at the

concentrations studied. The LiOH base, used in PWR to control the pH of water, seems to have a negative effect on water decomposition, although we cannot fully explain the origin of this result. In this case, the utilization of <sup>10</sup>B-EBA is preferable to NBA because it can allow to dissolve a lower amount of LiOH to control the pH of water.

#### Acknowledgements

The authors thank Dr L. Gilles, head of the Department of the Experimental Reactors (CEA/DRN/DRE), for authorizing the numerous irradiations at the ISIS facility. These experiments would not have been possible without the technical assistance of Dr H. Carcreff and Mr G. Uzureau. Dr Y. Frongillo has contributed to this paper for the calculations of the dose in the irradiated ampoules. The authors are also grateful to Dr D. You and to Dr D. Feron at the CEA/DTA/SCECF laboratory for supplying the pH data with the MULTEQ® code.

#### References

- [1] B. Pastina, Phd thesis Ref. 4862, Université de Paris-Sud (1997).
- [2] C.J. Wood, W.J. Marble, M. Prystupa, M.J.B. Hudson, D. L. Wilkens, International Conference on Water Chemistry in Nuclear Reactor Systems 5, Bournemouth, UK, 23 October–27 October 1989 (BNES, London, 1989).
- [3] A.O. Allen, J. Hochanadel, J.A. Ghormley, T.W. Davis, J. Phys. Chem. 56 (1952) 575.
- [4] B. Pastina, J. Isabey, B. Hickel (submitted for publication in Radiat. Phys. Chem. (1998a)).
- [5] B. Pastina, J. Isabey, B. Hickel (submitted for publication in Radiat. Phys. Chem. (1998b)).
- [6] A.O. Allen, The Radiation Chemistry of Water and Aqueous Solutions, Van Nostrand, New York, 1961.
- [7] E.J. Hart, W.R. McDonnell, S. Gordon, International Conference Peaceful Uses of Atomic Energy, Geneva, Suisse, 6 August–20 August, 1955, vol. 7, p. 593 (United Nations, New York, 1956).
- [8] C. Brun, A. Long, P. Saurin, M. C. Thiry and N. Lacoudre, Int. Conf. Chemistry in Water reactors: Operating Experiences and new Development, Nice, France, 24 April–27 April 1994, (SFEN, Paris, 1994).
- [9] K. Ishigure, N. Fujita, T. Tamura, K. Oshima, Nucl. Technol. 50 (1980) 169.
- [10] A.B. Ross, W.G. Mallard, W.P. Helman, G.V. Buxton, R. E. Huie, P. Neta, NDRL-NIST Solution Kinetics Database: version 2.0, NIST, Gaithersburg, USA, 1994.
- [11] B. Chen, R. Pathania, C.J. Woods, PWR primary water chemistry guidelines. Revision 3, EPRI Report 105-714 (1995).
- [12] M.V. Polley, H.E. Evans, International Conference on Water Chemistry in Nuclear Reactor Systems 6, Bourne-

- mouth UK, 12 October– 15 October 1992 (BNES, Londres, 1992).
- [13] G.V. Buxton, in: Farhataziz, M.A.J. Rodgers (Eds.), *Radiation Chemistry. Principles and Applications*, VCH, New York, 1987, p. 321.
- [14] A.J. Elliot, Rate constants and G-values for the simulation of the radiolysis of light water over the range 0-300°C, Atomic Energy of Canada Limited Report, AECL - 11073, COG-94-167 (1994).
- [15] H. Christensen, *Nucl. Technol.* 109 (1995) 373.